

IUE DATA REDUCTION

## XXV. Implementation of Basic Improvements to Extraction of High Dispersion Spectra

Ralph C. Bohlin and Barry E. Turnrose

SUMMARY

The new software package for extraction of high-dispersion IUE spectra has been implemented in production data processing, effective on Nov. 10, 1981. The photometric correction of IUE images in high dispersion is now done with the same technique used in the new low-dispersion software, which became operational on November 3, 1980 at NASA and on March 10, 1981 at VILSPA. As is the case in low dispersion, the single most important improvement in high dispersion is an increase in apparent resolution, achieved by doubling the number of points at which a spectrum is sampled. Numerous other benefits are found in the new software, which improve the quality of the extracted data and make its interpretation more straightforward. For example, a variable slit height is used for the data extraction to optimize the photometry and signal-to-noise at each order, wavelengths are corrected for the motion of the earth and the IUE satellite to a heliocentric reference frame with air wavelengths used consistently longward of 2000A, the essential documentation in the headers is expanded, and the flagging of anomalous data points is upgraded.

## I. INTRODUCTION

The new software in low dispersion is described by Bohlin, Lindler, and Turnrose (1981) and Turnrose, Bohlin, and Lindler (1981). The photometric correction in high dispersion is now done using an implicit geometric correction rather than the explicit techniques of the old software, just as is the case for low dispersion. The photometrically corrected image is in the original distorted frame of the raw image. The full resolution is still preserved and the noise can be treated uniformly rather than being suppressed non-uniformly by the old bi-linear interpolation used to resample the data onto the square grid of 13 x 13 reseaux. In order to extract the spectral information, the dispersion constants for the geometrically correct space are implicitly adjusted for the known distortion in the IUE cameras in order to associate the correct wavelengths with a spectrum in the distorted frame of reference. A measurement of the spectral flux is extracted for every diagonal row of pixels, which are all within  $10^0$  of the perpendicular to the dispersion direction. The old software sampled only half as often with an effective slit width double the 0.7 pixel (1 pixel = 37  $\mu$ m) spacing of the new software. The old extraction had a non-uniform spacing, where about every fifth point was spaced only by one-half the normal amount and also resampled part of the same data represented in the previous point.

During the course of this revision to the IUE production software, it has been possible to incorporate several improvements into the old high dispersion extractions. Only the difference between the old software, as it now stands,

and the new software will be discussed here. In order to make the old versus new comparisons, the old data has been reprocessed with all the improvements in that system, so that the reader should exercise caution in interpreting old data on the basis of the quality of reprocessed spectra. A detailed history of past changes to IUE production software is in Turnrose and Harvel (1982) and Turnrose, Harvel, and Mallama (1982). For some details of the new software not covered here see Lindler and Bohlin (1980). Section II contains the documentation of the improvements in apparent resolution; and Section III details the optimization of the new slit heights, which vary with order number. Section IV quantifies the increase in noise that has accompanied the removal of the artificial smoothings of the old extractions and explains the effects of two recommended filters. The verification of the photometric properties of new spectra relative to old spectra is in Section V. Finally, Section VI summarizes the other improvements realized with the new system.

## II. IMPROVEMENTS IN VISIBILITY OF NARROW FEATURES

A major advantage of the new software is an increased visibility of narrow features, achieved by avoiding the geometric resampling, by using a narrower slit width, and by more frequently sampling the spectral image. Figure 1 illustrates the improvement seen in the case of closely spaced line pairs from a Pt-Ne spectrum of the IUE wavelength calibration lamp. Two emission lines are shown in each of three separate spectra for both cameras in order to demonstrate the basic consistency of the data. The improvement in resolvability is more marked in LWR; but in all cases, the peaks are higher and the valleys between the emission lines are lower in the new extractions.

### A. Special Warning on Correlated Camera Noise

The point-to-point noise is increased somewhat by the new software as expected because of the omission of the filters applied in the old software (see Section IV). However, another problem arises occasionally that was effectively masked by the old reduction but can be seen clearly in the SWP 10253 spectrum in the 1493 $\text{\AA}$  region as a tremendous oscillation of the signal by about  $\pm 100$  percent. The original data image suggests the presence of an electronic instability, because a number of pixels along one diagonal are all heavily exposed (black). Along the adjacent diagonal lie lightly exposed pixels, and this pattern of light and black diagonals repeats. One can imagine the following explanation for this unfortunate situation, where the readout beam of the SEC vidicon has suffered a perturbation perpendicular to the scan path. The readout will be light on an upward swing and black on the downward. On the next scan line down in the readout, there will be excess charge where the previous scan oscillated up and a deficiency where the downward motion of the perturbation encroached on the normally undisturbed charge of the next line. Hence, the observed pattern in the image is created and is most evident in the adjacent diagonals of an extracted spectrum.

An astronomer will often be able to recognize the camera noise as a checker-board pattern on the photowrite image with a different spatial extent than the spectrum of the target object. Various filters can be used to improve the cosmetic appearance of the correlated camera noise at the expense of some

resolving power in unaffected regions of the spectrum. Figure 2 shows the effect of two different filters on the correlated noise of SWP 10253 and the completely resolved line in LWR 8918. One filter is a two point average of every pair of points plotted at the average wavelength. This is equivalent to extracting the data with an artificial slit of twice the width and is similar to the old software, but with less smoothing and a higher sampling frequency. The other smoothing shown in Figure 2 is for the narrower "optimal" filter of Section IV. The optimal filter does not appreciably degrade the resolvability from that of Figure 1, but a filter as wide as two points is needed to significantly suppress the correlated camera noise.

### III. OPTIMAL SLIT HEIGHTS

The old software extracts spectra from the IUE image with a fixed artificial slit of effective height of about 6.4 pixels for point sources and 9.2 pixels for extended sources, while the new slit heights are allowed to vary with order number to account for changes in the width, separation, and residual geometric distortion ("wiggles") of each order. For point sources, the slit height should never exceed the order separation, which reaches a minimum of 5.25 pixels in SWP (Turnrose and Bohlin 1979). Where the orders are well separated, the optimal slit height is determined by the trade-off between excessive noise and photometric precision. The considerations in determining the optimal slit heights for the new software are outlined below for the separate cases of point and extended sources.

#### A. Point Sources

The underlying principle guiding the determination of the slit height is that the shortest slit compatible with a reasonable photometric stability should be used. The use of short slits minimizes the contamination of the gross spectrum by background noise, a fact which is particularly significant for long exposures and weak signal levels, where the effect of bright spots falling within the extraction slit is the worst. On the other hand, the use of slits which are too short exacerbates the sensitivity to irregularities in IUE images and compromises the photometric stability. Such irregularities include the variation in the width of the high dispersion orders. Schiffer (1980) shows the full width at half maximum (FWHM) of the echelle orders in SWP point source spectra to differ by at least a factor of 1.5, where the long wavelength (low) orders are the widest. A second irregularity is that the orders are not truly straight but possess "wiggles" even after the geometric correction with temperature effects removed (Thompson, Turnrose, and Bohlin 1982). The third irregularity is residual differential registration perpendicular to the dispersion direction; i.e. if the orders at one part of the tube are perfectly registered with the dispersion relations, the orders at distant parts of the tube may be misregistered by amounts as large as ~0.5 pixel in a way which is systematic with order number but variable in sign and amplitude from image to image.

The approach taken in the new software is to register the images accurately in the short wavelength regions of the higher, more closely spaced orders, where slit heights are limited by the order separation and where the level of the

extracted background signal is critically dependent on the registration. To compensate for the three limiting factors (order width, wiggles, and differential shifts) at the lower orders, the slit heights are increased.

To determine the proper slit heights, a series of tests was conducted on the image SWP 10306, a 6 second exposure through the large aperture of the star eta UMa. Extractions were made with a number of slit heights ranging between 5 and 8 pixels and with registered and misregistered ( $\pm 0.4$  px) extractions to simulate the effects of variable, differential registration. In analyzing the data, net spectra were binned into contiguous segments, typically 9 such bins per order. The shortest slits are identified consistent with the constraint of a maximum photometric error of 3 percent in any single bin between registered and misregistered extractions. Figure 3 illustrates the observed behavior of the 8 bins used for order 68 in SWP 10306. As can be seen, the effects of signal loss due to misregistration increase with decreasing slit height. At the high orders ( $\sim 100$  and higher) the behavior (not illustrated) is different, with little change with slit height but drastic changes with registration due entirely to changes in the derived background level. Particular attention was paid to those low orders known to exhibit substantial wiggles. The final slit heights chosen increase linearly from a value of 5 pixels at order 125 to 7 pixels at order 68, and then linearly to a value of 10 pixels at order 66. These heights are sufficiently liberal to allow for the behavior of those orders not explicitly analyzed and to allow for unexpectedly severe differential registrations. Therefore, the photometric precision of extracted spectra should not be compromised by more than 3 percent by our choice of slit heights. These slit heights have been adopted for use in both the SWP or LWR cameras, point-source reduction mode, and supercede the unnecessarily long slits originally planned for the new software (Turnrose and Bohlin 1979). Note that for orders 86 to 125, the new slit height is less than that (6.4 pixels) used by the old software, and for orders 66 to 85, the new slit height is greater than the old.

## B. Extended Sources

In the case of extended sources, similar considerations apply, although the width of the large aperture perpendicular to the dispersion ( $\sim 7$  pixels) necessitates a different approach to the problem of choosing the slit heights at the closely spaced orders. The need to keep the slit height shorter than the order separation is outweighed by the need to measure substantially all of the flux, particularly since many extended objects are emission-line sources for which continuum contamination from adjacent orders is unimportant.

Analyses similar to those described in section III A were performed for a series of slit heights ranging from 6 to 11 pixels. The primary data were obtained from 100-minute exposures of the Orion Nebula, SWP 10744 and LWR 9427, for which nebular continuum is present. From these data, a constant slit height of 10 pixels for all orders was chosen. This value is slightly larger than the 9.2-pixel slit used in the old software; extending the slit to 11 pixels increases the measured net signal by less than 1 percent. As a check, the net emission line fluxes from the L<sub>α</sub> sky background and the lines of the planetary nebula NGC7662 were analyzed on SWP 6468 and LWR 5546 to corroborate the choice of a 10-pixel slit height. Note that this choice of a constant 10-pixel slit height for extended sources differs from the slit originally proposed in Turnrose and Bohlin (1979).

## IV. NOISE CHARACTERISTICS

### A. Comparison of New Software with Old Software

As mentioned in earlier sections, the old IUE reduction software performed an explicit geometric correction consisting of a bi-linear resampling to map the raw pixels onto a grid in which the reseau marks are corrected to the proper square grid. One problem with this technique is that pixel-to-pixel noise is smoothed, non-uniformly. In some portions of the image, the resampling falls on pixel centers, and in other portions of the image, the resampling falls between pixels. In the former locations, the raw sample values are unchanged, whereas in the latter regions, the smoothing suppresses the high frequency noise. Because some regions of the IUE detectors have little geometric distortion and because the image is resampled to the same nominal size, the phase of the bi-linear resampling changes slowly with respect to the pixel size, thus producing alternating bands of noisy and smoothed data in a geometrically corrected image. This non-uniform signal-to-noise is particularly objectionable, because very smooth spectral regions might mislead an investigator into falsely identifying noise in unsmoothed regions as a spectral feature, especially in the presence of the correlated camera noise discussed in section II A. Settle (1981 private communication) has estimated that the expected reduction in apparent signal-to-noise ratio due to the elimination of the explicit geometric correction is approximately a factor of 1.5 on the average.

In addition, the fact that the old software utilized an extraction slit wider than that of the new software leads to a further increase in the point-to-point noise in the new software compared to the old, with a decrease in signal-to-noise by a factor of 1.6 as estimated by Settle. The combination of both effects leads to a total expected reduction in apparent signal-to-noise of  $\sim 2.4$  with the new software. Although this increase in noise might seem like a high price to pay for the increase in apparent resolution, the old software artificially inflated the apparent signal-to-noise ratio of the data in an obscure manner. Now, a spectrum can be smoothed straightforwardly by the use of a filter appropriate for any particular problem..

Actual numerical comparisons of the apparent signal-to-noise ratios obtained with the old and new software have been made by examination of the central portions of net ripple-corrected spectra of eta UMa. Noise-to-signal ratios (NSR), defined to be the percent scatter of the individual net ripple corrected flux points within a bin several angstroms wide, were calculated for representative orders between 83 and 118 with both the old and new software. The ripple corrected fluxes were used to avoid increasing the scatter due to a slope in the continuum, although the bins selected are very near the blaze peak. Bins affected by reseau marks or absorption lines are not considered, as they would tend to have an unusually large scatter in the fluxes. Table 1 summarizes the results for images SWP 10306 and LWR 3767. As expected, the signal-to-noise ratios typical of the new software are less than those of the old software by about a factor of 2.

Table 1

Comparison of Noise-to-Signal Ratios Obtained with New and Old Software

Image	Exposure Time (sec)	Aperture	$\frac{\text{NSR}^* \text{ (New)}}{\text{NSR} \text{ (Old)}}$
SWP 10306	6	large	1.83
LWR 3767	9	small	2.04

\*Noise-to-Signal Ratio (NSR) as defined in text.

### B. Noise-conditioning Filters

Whereas the old software artificially suppressed the point-to-point noise in extracted spectra, the new software does not. In particular, the correlated camera noise described in section II A is essentially preserved in the new extraction procedure. Schiffer (1981 private communication) has demonstrated that this camera noise has a characteristic power spectrum which dominates the observed power spectrum of the extracted data at high spatial frequencies. This high-spatial frequency noise might be conditioned, in order to judge the true noise characteristics of the actual spectral data. Filtering the extracted data with a 2-point filter (see Figure 2) has the appeal of strongly suppressing the correlated camera noise. Such a broad filter significantly affects the resolving power but is still not as much smoothing as is inherent in the old software.

Another approach is to treat the extracted data points with an "optimal" filter, constructed so as to flatten the power spectrum beyond the point at which the observed power spectrum reaches a minimum, i.e. for spatial frequencies greater than the maximum which is characteristic of the actual spectral data, about 0.25 cycles per pixel. Dr. F. H. Schiffer has derived such a filter from composite power spectra of 5 SWP and 5 LWR images for each camera separately. The optimal filters are to be applied in direct convolution with the extracted flux points. Table 2 lists the filter weights, from which it is seen that the filters are narrower than the two-point binning filter discussed above. In practice, the effect of the 7-point filters differs little from that of the renormalized central three points alone, because the four points in the wings have a weight well below that of the photometric precision. Presently, the optimal filter for the LWP camera has not been determined, so that data is unfiltered.

Table 2

## Optimal Filter Weights

Element No.	Element Value		LWP
	LWR	SWP	
1	0.0016	-0.0021	0
2	0.0018	-0.0060	0
3	0.0602	0.1017	0
4	0.8728	0.8128	1
5	0.0602	0.1017	0
6	0.0018	-0.0060	0
7	0.0016	-0.0021	0

Table 3 summarizes the quantitative noise characteristics of spectra filtered with the optimal filters of Table 2, compared again to the results of the old software as in Table 1, but with two additional eta UMa exposures. These data indicate that the optimal filtering reduces the high frequency noise in extracted net ripple corrected spectra by approximately a factor of 1.2, resulting in a noise-to-signal ratio near what would be expected by just reducing the old slit width by a factor of 2. Therefore, the net ripple corrected spectrum on magnetic tape and on Calcomp plots is filtered with the optimal filter. The gross and net spectra are left unfiltered, so that the astronomer can choose the best filter for any specific application.

Table 3

## Comparison of Noise-to-Signal Ratios Obtained with New Software (Optimally Filtered) and Old Software

Image	Exposure Time (sec)	Aperture	$\frac{\text{NSR}^* \text{ (New)}}{\text{NSR} \text{ (Old)}}$
SWP 10306	6	large	1.48
SWP 10522	6	large	1.38
LWR 3767	9	small	1.75
LWR 9210	6	large	1.50

\*As in Table 1

## V. PHOTOMETRY

Figure 4 compares the total net flux in IUE FN units as extracted by the new software to that extracted by the old system. The comparison spectra are processed with the same dispersion constants in both reductions. The mean flux in the same wavelength intervals is computed for every fifth order of the

echelle spectrogram avoiding both edges of the cameras by about 10 percent of the free spectral range. The ratios of NEW/OLD net flux in Figure 4 show a scatter of up to 4 percent about unity for the long wavelength (low) orders. The new fluxes are systematically greater by ~10 percent in the high orders, due to the lower background found between the close orders when the explicit geometric correction is omitted.

While Figure 4 shows the mean changes with order, Figure 5 addresses the question of changes within a given order. The observed free spectral range for the orders 108 and 88 is divided into 9 bins, and the ratio of extracted flux is plotted against the wavelength of each bin. Again the lower order ( $m = 88$ ) shows a small scatter about unity for both cameras with no significant systematic trends. The ratios for the higher order ( $m = 108$ ) are all greater than unity because of the lower backgrounds found by the new software. The small systematic slope to the flux ratios within  $m = 108$  are again due to a systematically lower extracted background as a fraction of the net with the new software at the shorter wavelengths (upper left region of SWP). This effect could be caused by an intrinsic broadening of the orders near the tube edge, thus enhancing the additional degradation suffered in the geometric correction of the old software.

In summary, the only significant change in the photometry of the new high dispersion software is an increase in extracted flux for the closer orders. This increase has reduced the amount of order overlap caused by excessively high backgrounds in the old software and should result in a ripple correction that is closer to theoretical expectations.

## VI. ADDITIONAL BENEFITS

In addition to the above improvements in apparent resolution, noise characteristics, and photometry, other advantages of the new software are itemized below.

1. All saturated pixels (DN = 255) are now flagged in the same way as in the new low dispersion software.
2. Reseau marks are narrower because there is no geometric correction to broaden them and because they do not grow in the process of subtracting the background, as was the case for the old processing.
3. All of the spectral data are sampled exactly once where each extracted data point is derived from independent pixels in the raw image.
4. The dynamic range of extrapolation in the ITF is expanded and this extrapolation is flagged in analogy with low dispersion.
5. Reseaux, microphonics noise in LWR, and saturated pixels are not used in the background computation and are, therefore, not flagged in the background.
6. The wavelengths are corrected to a heliocentric coordinate system and are converted to air wavelengths consistently for both cameras longward of  $2000\text{\AA}$ .
7. More information such as the observing date, target coordinates, and dispersion constants are included in the data header (record zero), as is now the case in low dispersion.



## ACKNOWLEDGEMENTS

The new high dispersion software was written by D. J. Lindler of Andrulis Research Corp. R. W. Thompson, B. T. Coulter, and A. D. Mallama of Computer Sciences Corp. participated in the analysis of the data presented here. R. Thompson is responsible for the implementation and maintenance of all IUE production software.

## REFERENCES

Bohlin, R. C., Lindler, D. J., and Turnrose, B. E.: 1981, "IUE Data Reduction XIX. Results of Basic Improvements to the Extraction of Spectra from IUE Low Dispersion Images," NASA IUE Newsletter No. 12, p. 9, also in IUE Data Reduction, ed. W. W. Weiss, et al. (Vienna: Austrian Solar and Space Agency), p. 1 and in IUE ESA Newsletter No. 10, p. 10.

Lindler, D. J., and Bohlin, R. C.: 1980, in IUE Data Reduction, ed. W. W. Weiss, et al. (Vienna: Austrian Solar and Space Agency), p. 21.

Schiffer, F. H. III: 1980, "Order Width in High Dispersion," Report to IUE Three Agency Coordination Meeting.

Thompson, R. W., Turnrose, B. E., and Bohlin, R. C.: 1982, Astron. Ap., (in press).

Turnrose, B. E., and Bohlin, R. C.: 1979, "IUE Data Reduction VIII. Planned Changes to the High Dispersion Extraction Slit Height," NASA IUE Newsletter No. 6, p. 195.

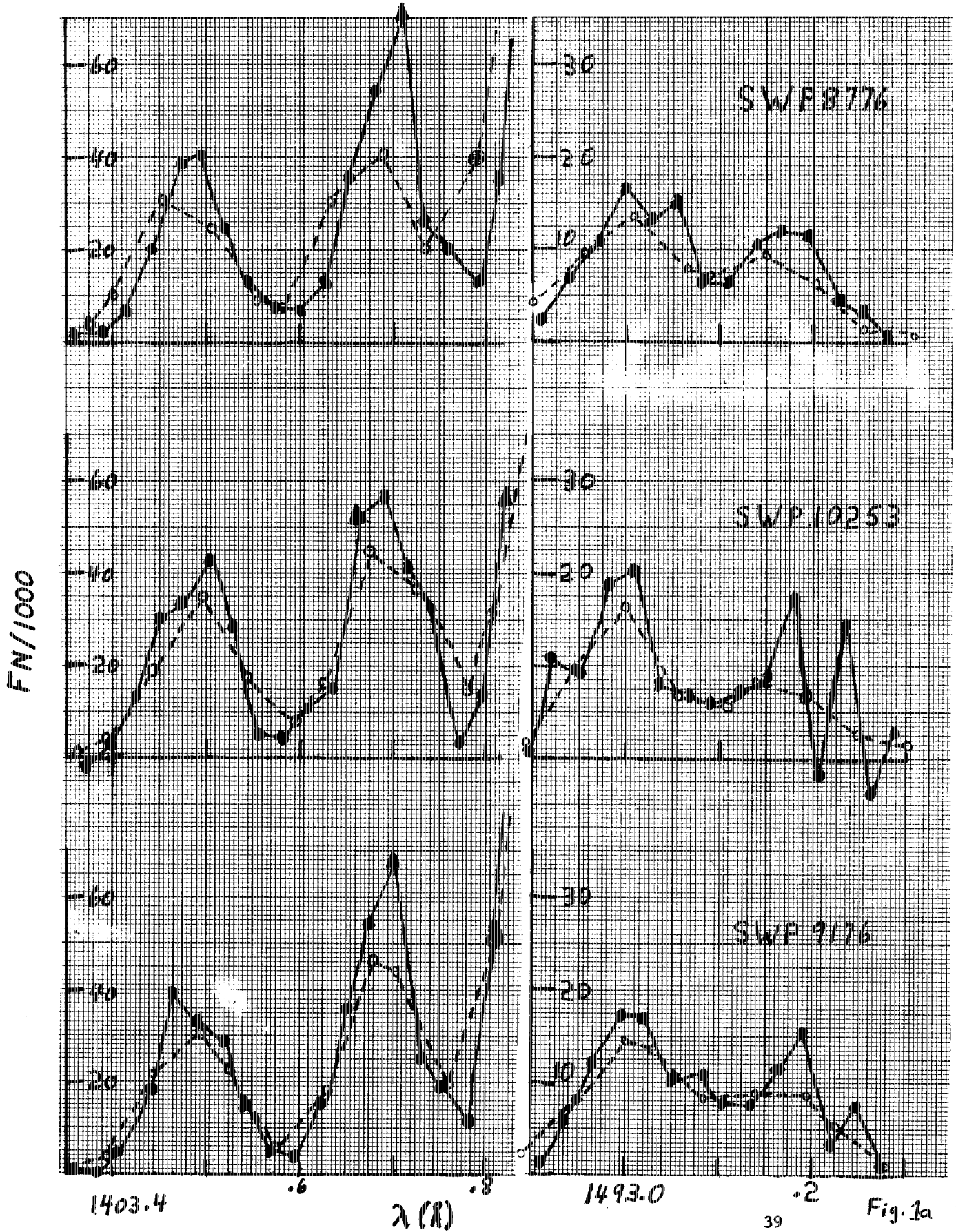
Turnrose, B. E., Bohlin, R. C., and Lindler, D. J.: 1981, "IUE Data Reduction XVIII. Implementation of New Low Dispersion Software: Summary of Output Format Changes," NASA IUE Newsletter No. 12, p. 2.

Turnrose, B. E., and Harvel, C. A.: 1982, "Techniques of Reduction of IUE Data: Time History of IUESIPS Configurations," NASA IUE Newsletter No. 16.

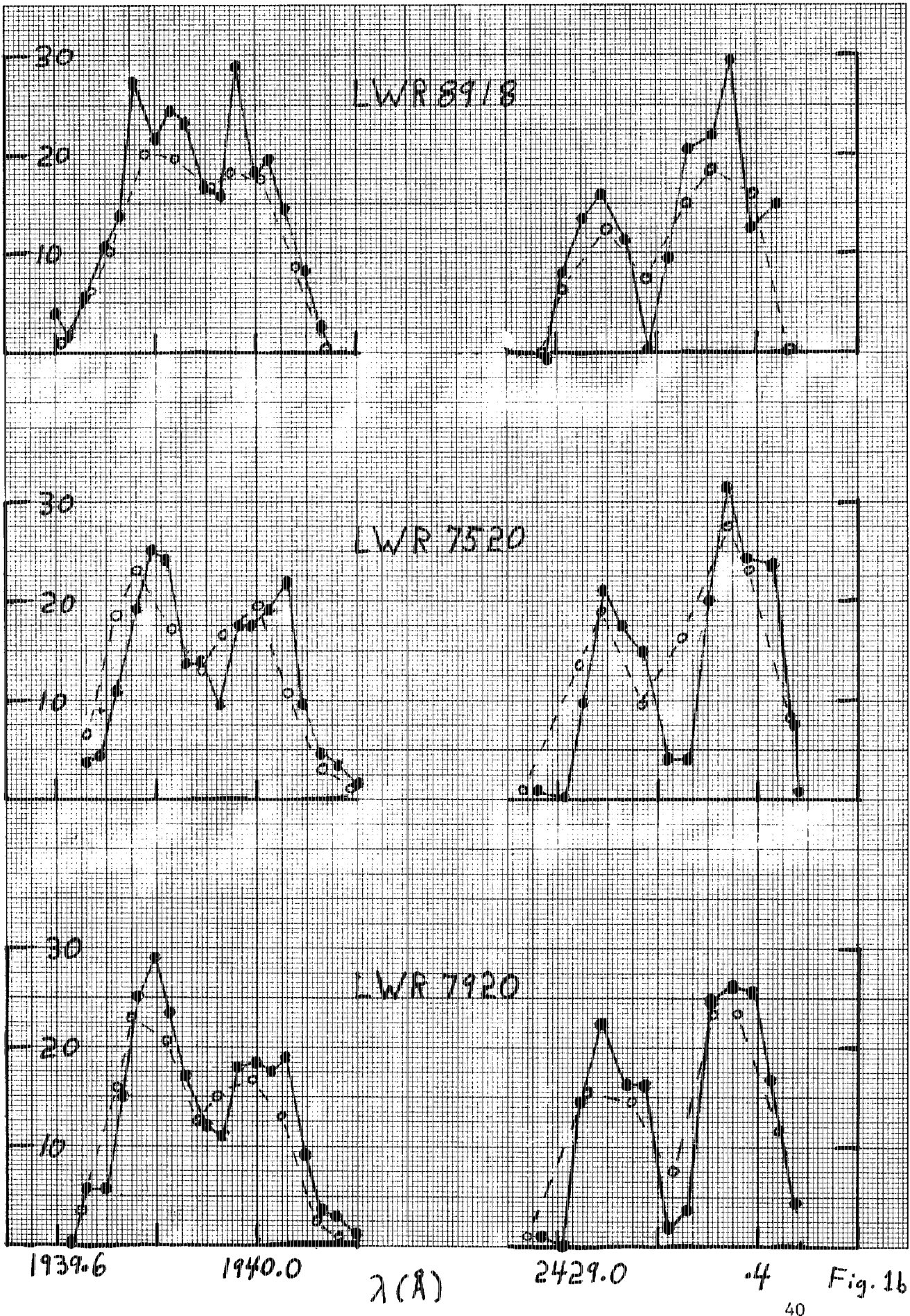
Turnrose, B. E., Harvel, C. A., and Mallama, A. D.: 1982, "Techniques of Reduction of IUE Data: Methods for Improving Previous IUESIPS Tape Products," NASA IUE Newsletter No. 17.

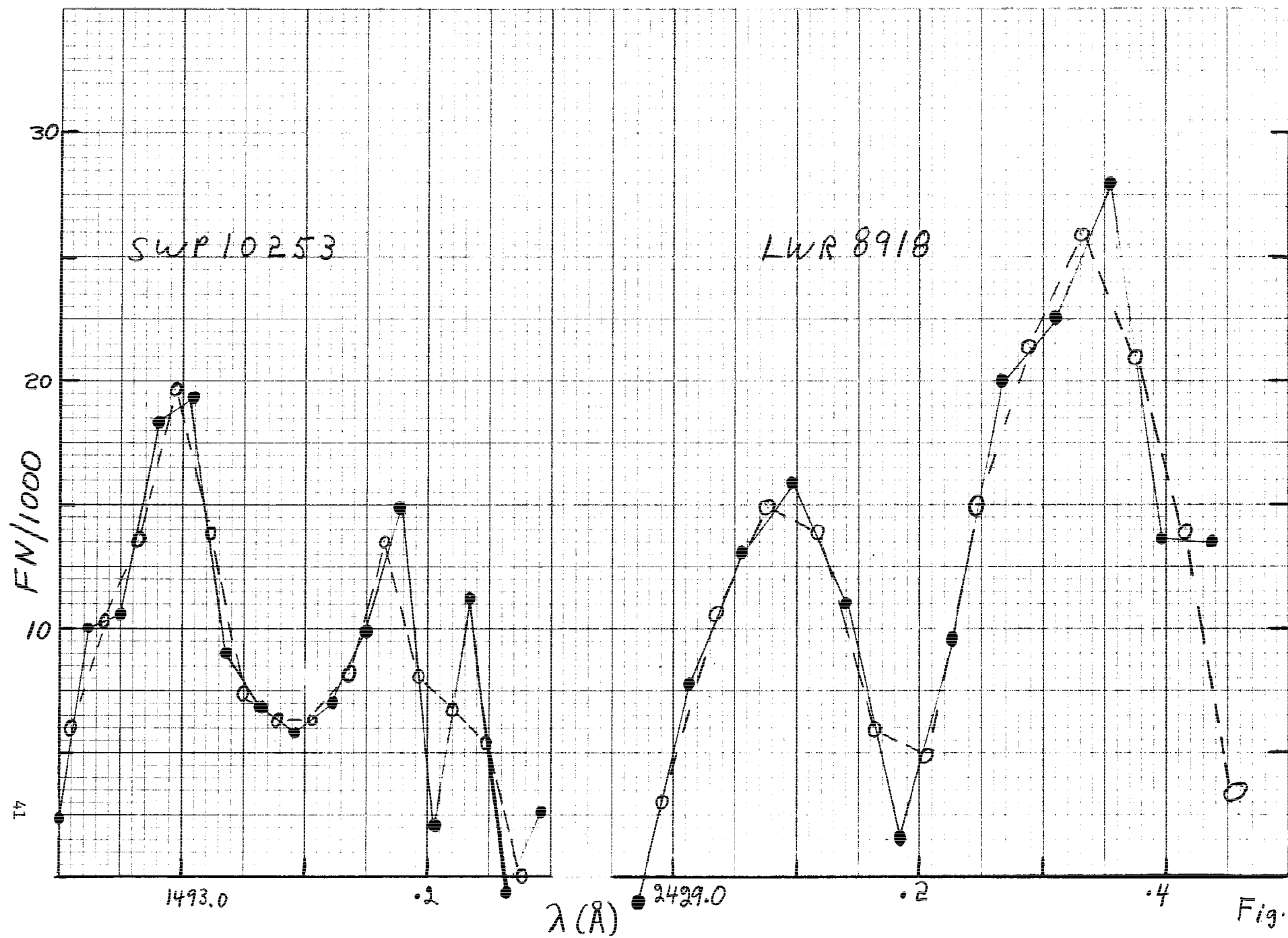
## FIGURE CAPTIONS

- Fig. 1 - Close pairs of emission lines from the IUE Pt-Ne lamp for (a) the SWP camera and (b) the LWR camera. The filled circles are extracted by the new software, while the open circles are from the old software. The few triangles are cases of extrapolation in the ITF that are now flagged by the new software.
- Fig. 2 - A comparison of a two point filter (open circles) and an optimum noise reduction filter (filled circles) for two of the line pairs of Fig. 1. Note that the two point filter effectively eliminates the camera noise in the SWP data but does cause significant blending of the LWR line pair.
- Fig. 3 - Percentage changes in net signal as measured in 8 contiguous  $2\text{\AA}$  bins in order 68, SWP 10306, as functions of both slit height and registration accuracy. The percent deviation is relative to a zero level for the net flux as measured with a centered, 7-pixel high slit. The slit height in pixels is noted near the ends of pairs of curves, where the continuous lines connect the filled circles derived for a centered extraction and broken lines connect the open circles derived from an extraction intentionally misregistered by 0.4 pixel. Note the color changes and local anomalies induced by a misregistration of 0.4 pixels when a short slit is used.
- Fig. 4 - Ratios of total <sup>net</sup> flux extracted by the new to that of the old software as a function of echelle order number. Ratios for two spectra from each camera are shown.
- Fig. 5 - Ratios of new to old flux within echelle orders 108 and 88 for both cameras. The bandpass for each data point is  $1.78\text{\AA}$  in 108 and  $2.67\text{\AA}$  in 88 for SWP and  $3.26$  and  $4.58\text{\AA}$ , respectively, for LWR.

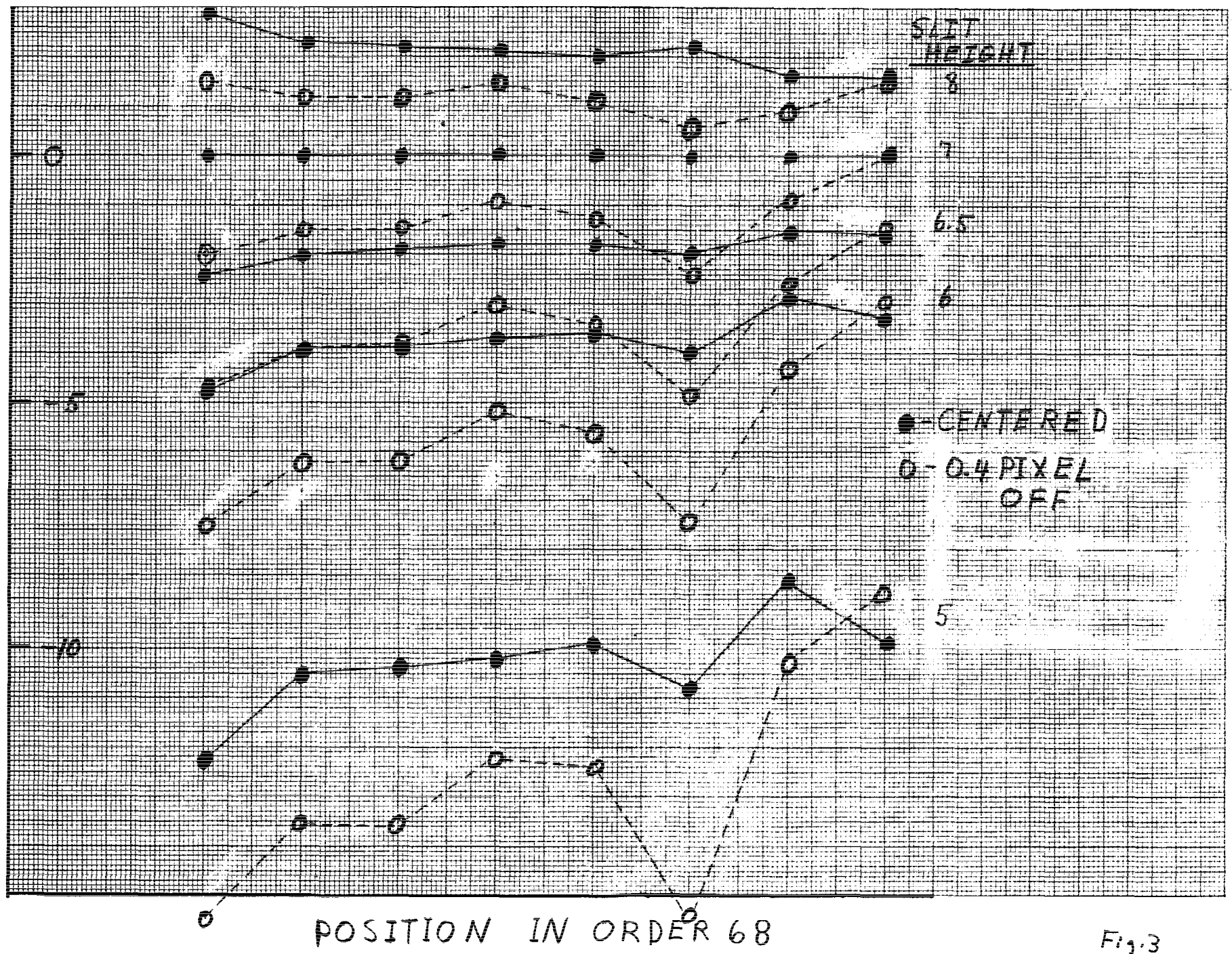


$F_N/1000$





% DEVIATION



POSITION IN ORDER 68

Fig. 3

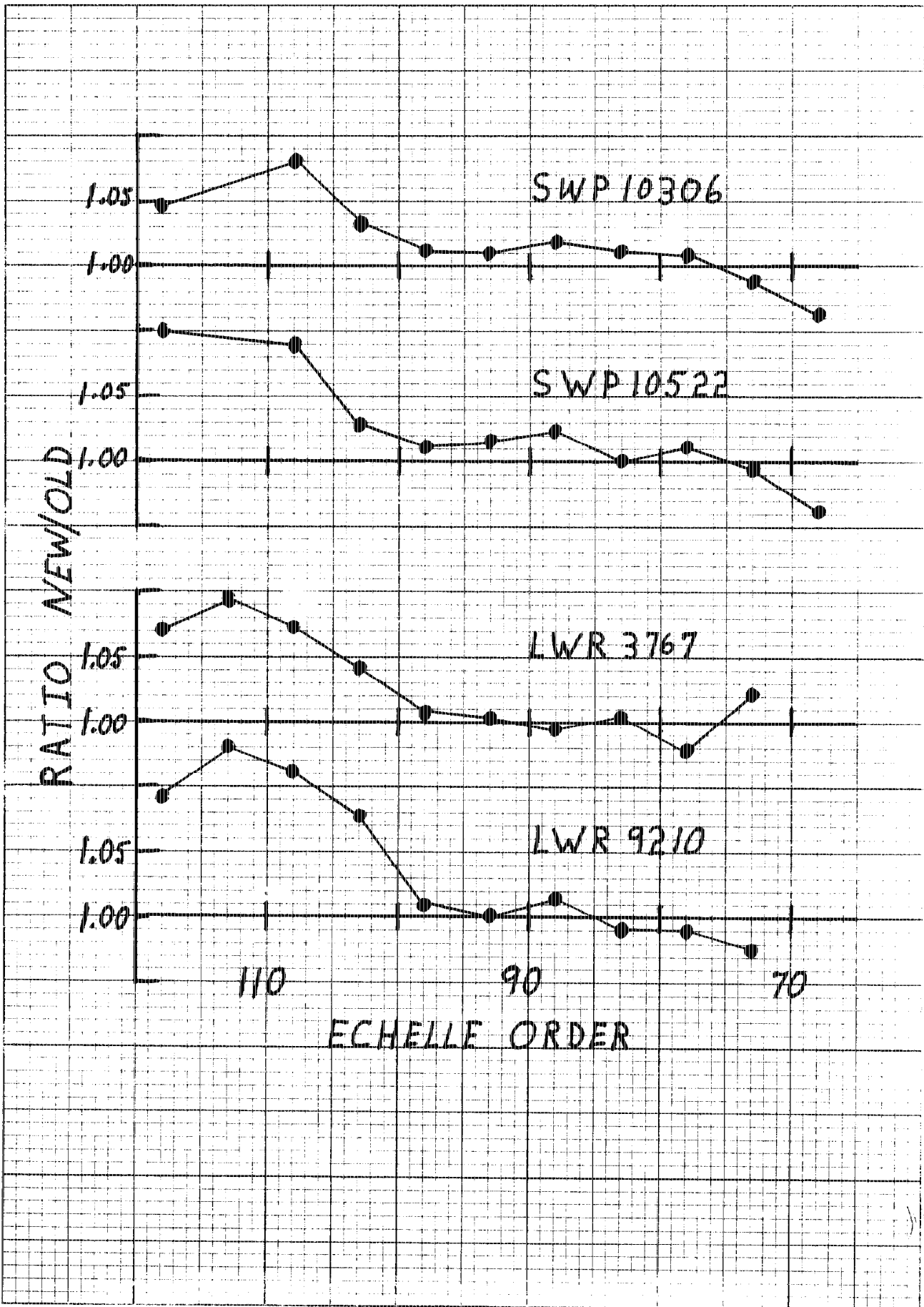
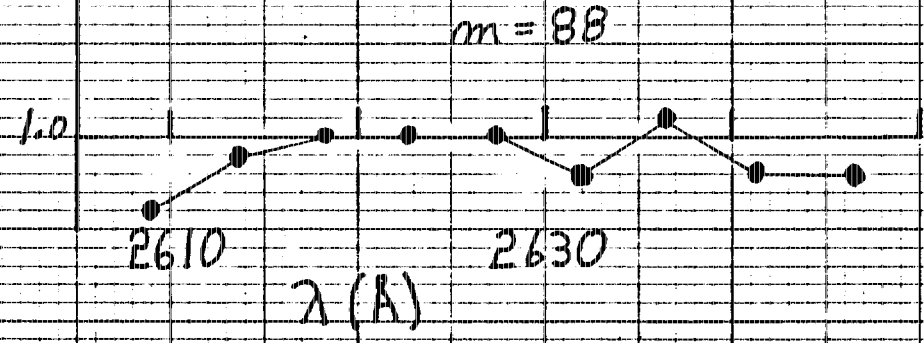
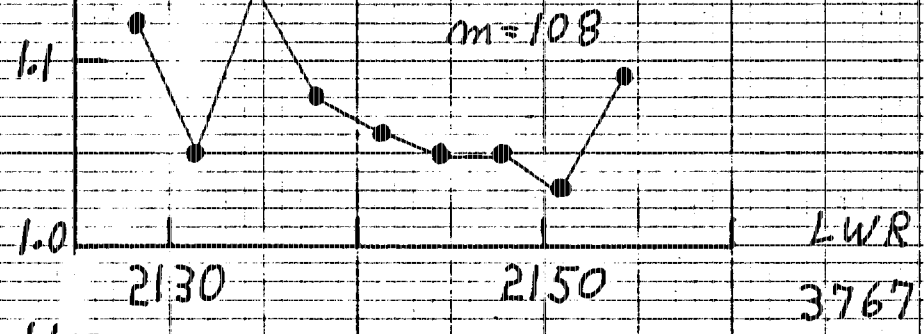
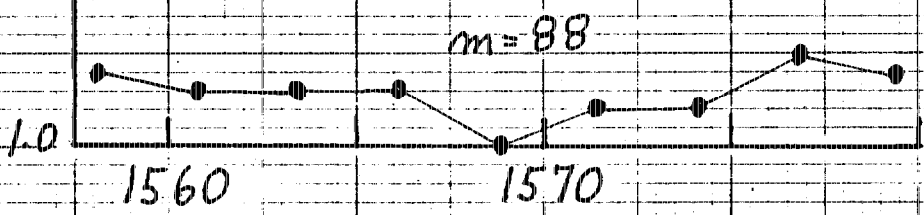
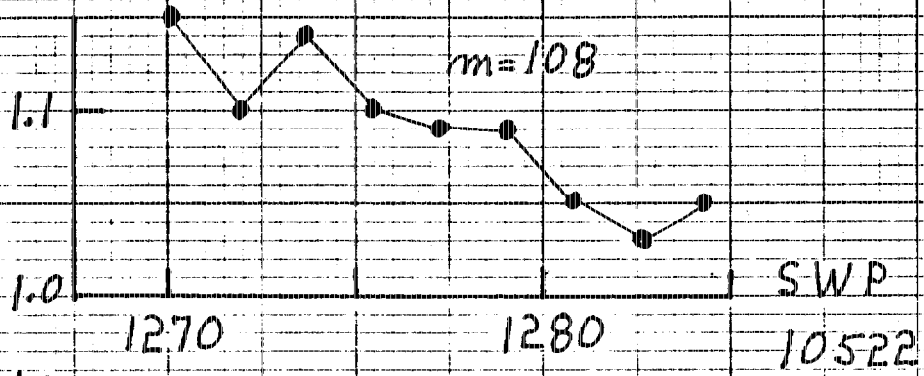


Fig. 4

RATIO NEW/OLD



$\lambda(A)$

Fig. 5